PHYSICAL REVIEW B VOLUME 60, NUMBER 3 15 JULY 1999-I

Reconstructions of the Si-terminated (100) surface in β-SiC: A theoretical study

R. Gutierrez, M. Haugk, and J. Elsner
Theoretische Physik III, Institut für Physik, Technische Universität, D-09107 Chemnitz, Germany

G. Jungnickel, M. Elstner, A. Sieck, and Th. Frauenheim
Universität GH Paderborn, Fachbereich Physik, Theoretische Physik, D-33098 Paderborn, Germany

D. Porezag
Complex Systems Theory Branch, Naval Research Laboratory, Washington, D.C. 20375-5345

(Received 1 December 1998)

Using a self-consistent-charge density-functional based tight-binding approach the structural properties and relative stabilities of Si-terminated reconstructions of the (100) surface in β-SiC are discussed. All low-energy surfaces are found to be semiconducting. Over a wide range of growth conditions a model with 2×3 periodicity has a low formation energy. Only in a Si-rich environment does a 3×2 structure become stable. [S0163-1829(99)04824-9]

I. INTRODUCTION

Silicon carbide possesses a variety of interesting physical properties such as its chemical inertness, high electron mobility, high thermal conductivity, and the capability of withstanding high temperatures, which makes it a promising candidate for application in high-temperature, high-frequency, and high-power electronic devices.[1]

During the past decade the properties of cubic and some hexagonal polytypes of bulk SiC have been extensively studied by *first principle* approaches.[2–5] With regard to the structural properties of SiC surfaces empirical and semiempirical calculations[6–15] have been performed. Moreover, in recent years, accompanied by the increasing interest in silicon carbide, a number of studies on an *ab initio* basis has also appeared discussing a variety of reconstruction models for, e.g., (100) and (111) surfaces in the cubic phase[16–23] as well as for the (0001) surface in the 6H hexagonal phase.[24–27]

By processing chemical vapor deposition using alternating exposure of the surface to hydrocarbon and silane-rich gas phases the (100) and (111) faces of β-SiC have been grown.[28–31] The full-coverage Si-terminated (100) surface appears in (2×1) or $c(4\times2)$ symmetries which have usually been interpreted in terms of asymmetric dimers, analogously to Si surfaces.[32] In the presence of excess silicon at increasing concentration and after long-time exposure to Si_2H_6, 3×2, 5×2, and 7×2 reconstructions have been observed, too.[32–34] For the 3×2 surface reconstruction models with different Si coverage have been proposed by Yan, Smith, and Jonsson,[27] Hara *et al.*[33] and Dayan,[34] all of which basically consist of Si dimers on top of a silicon-terminated surface.

Carbon-terminated (100) surfaces are either produced by prolonged exposure to C_2H_2 (Ref. 31) or by a long-time annealing of the Si-terminated SiC surface at 1250 °C.[30] Similar to the related diamond counterpart this surface is stabilized by dimer formation, now developing, however, a staggered $c(2\times2)$ symmetry. For a more extensive account of the experimental situation on the (100) surfaces a recent review article of Bermudez[36] is referred to.

The situation for the full-coverage Si-terminated surface is quite unclear. Semiempirical methods[6–13] predict dimer formation with relatively short dimer lengths (~2.16–2.33 Å). On the contrary, though, various local-density-approximation–density-functional-theory (LDA-DFT) calculations[19,21] support a very weak dimerization with rather long bonds (2.73–2.75 Å) and no buckling at all. The *ab initio* results of Yan, Smith, and Jonsson[27] yield short dimer lengths ($d_{\text{Si-Si}}\sim2.26$ Å) while calculations performed with the same method by Catellani, Galli, and Gygi [22] rather support the LDA-DFT predictions ($d_{\text{Si-Si}}\sim2.58$ Å).

When considering Si-rich (100) surfaces, Yan, Smith, and Jonsson[27] report a 1/3 monolayer of excess silicon in an alternate row structure as the most stable surface upon comparison with the added-dimer-row model proposed in Ref. 33.

6H-(0001) surfaces have been investigated using, e.g., low-energy electron diffraction (LEED),[37] scanning tunneling microscopy (STM),[38] and other surface sensitive techniques (for a recent review see Martensson, Owman, and Johansson [39]) and 3×3, 1×1, and $\sqrt{3}\times\sqrt{3}$ reconstructions have been observed. For these surfaces several models have been proposed for the atomic arrangement. For the Si-terminated surface, Sabisch, Krüger, and Pollmann,[24] Northrup and Neugebauer,[25] and Käckell, Furthmüller, and Bechstedt[26] agree in that the Si adatoms placed on T4 positions provide the energetically most favorable structure, while for carbon termination Sabisch, Krüger, and Pollmann[24] determine a 1×1 structure consisting of a full monolayer of Si adatoms as the most stable configuration.

In the following we are going to apply a *self-consistent-charge density-functional* based *tight-binding* method (SCC-DFTB) to investigate the reconstruction of zinc-blende SiC (100) surfaces. We concentrate on Si-terminated surfaces only since for the C-rich surfaces there is now general agreement between theoretical predictions and experimental results (see, e.g., the review of Bermudez[36]). Moreover, in view of a future application of our method to the study of

0163-1829/99/60(3)/1771(6)/$15.00

TABLE I. Structural parameters of the (110) surface. Bond angles are defined as follows: $\alpha=(\mathrm{Si}^{\mathrm{sur}}-\mathrm{C}^{\mathrm{sur}}-\mathrm{Si}^{\mathrm{sub}})$, $\beta=(\mathrm{C}^{\mathrm{sur}}-\mathrm{Si}^{\mathrm{sur}}-\mathrm{C}^{\mathrm{sur}})$, and $\gamma=(\mathrm{C}^{\mathrm{sur}}-\mathrm{Si}^{\mathrm{sur}}-\mathrm{C}^{\mathrm{sub}})$.

		(110) 1×1 surface			
$d^{\mathrm{sur}}_{\mathrm{Si\text{-}C}}$ (Å)	$d^{\mathrm{sur\text{-}sub}}_{\mathrm{Si\text{-}C}}$ (Å)	α	β	γ	Method
1.821	1.897/1.87	98.16	118.2	115.6	SCC-DFTB
1.767	1.86/1.823	99.8	120.2	116.4	DFT-LDA (Ref. 20)
1.761	1.89/1.84	106	122	112	ASED (Ref. 10)

oxidation processes on Si-terminated SiC surfaces it is of interest to determine the range of stability of different reconstruction models at this termination. In the next section we briefly describe the computational approach. In Sec. III results for the (110) and (111) $\sqrt{3}\times\sqrt{3}$ surfaces are presented as a benchmark for our method. In Sec. IV we consider then different surface models for the (100) orientation at Si termination.

II. SIMULATION METHOD AND GEOMETRY

The interatomic potentials and forces are derived by means of a *density-functional* based nonorthogonal *tight-binding* scheme,[40] which has recently been improved by including a self-consistent calculation of the Mulliken charge distribution at each relaxation step.[41]

We model our surfaces within slabs periodic in two dimensions containing eight monolayers of SiC. The first five monolayers are allowed to relax whereas the atoms of the last three monolayers are fixed to preserve bulk symmetry. The dangling bonds at the bottom of the surface slabs are saturated with hydrogen. Four k points are used to sample the Brillouin zone.

Assuming thermodynamic equilibrium, the formation energies of surfaces can be expressed as a function of the chemical potentials describing the growth conditions:

$$E_{\mathrm{for}}=E-n_{\mathrm{C}}\mu_{\mathrm{C}}-n_{\mathrm{Si}}\mu_{\mathrm{Si}},$$

where E is the total energy of the supercell, n_i the numbers of each type of atoms in the cell, and μ_i the corresponding chemical potentials. According to Quian, Martin, and Chadi[42] the above expression can be simplified to

$$E_{\mathrm{for}}=E-n_{\mathrm{C}}\mu^{\mathrm{bulk}}_{\mathrm{SiC}}-(n_{\mathrm{Si}}-n_{\mathrm{C}})\mu_{\mathrm{Si}}. \qquad (1)$$

III. BENCHMARKS

Recent *ab initio* data on the (110) (Refs. 10,16, and 20) and (111) (Refs. 24–26) surface reconstructions provide a benchmark for applications of the SCC-DFTB method to SiC surfaces.

In accordance with predictions from the aforementioned studies for the (110) surface we find a buckling of the first surface layer. This buckling is driven by a charge transfer from the Si atom to the more electronegative C atom. This results in an emptied Si-derived dangling bond and a full lone pair localized at the C atom. Therefore the Si atom adopts an sp^2-like hybridization whereas the C atom moves outward into a p^3-like configuration. The resulting surface is therefore semiconducting. The details of the geometry found within the SCC-DFTB approximation are in good agreement with the self-consistent-field (SCF) LDA results[10,16,20] and are shown in Table I. Moreover we calculated a surface formation energy of 224 meV/Å^2, a value which agrees well with the reported *ab initio* result of 243 meV/Å^2.[5]

Concerning the (111) surface its reconstruction behavior should be expected to be similar to that of the (0001) surface of the 6H polytypes due to the similar surface topologies. A variety of experimental investigations has been reported for the latter (see, e.g., the review of Martensson, Owman, and Johansson [39]) concentrating mainly on the atomic structure of $(\sqrt{3}\times\sqrt{3})R30$ reconstructions. Recent calculations by Northrup and Neugebauer,[25] Käckell, Furthmüller, and Bechstedt,[26] and Sabisch, Krüger, and Pollmann[24] support the experimental conclusions that structures with Si adatoms placed on T4 or H3 positions are energetically favored. We have investigated the stability of different reconstructions with Si and C adatoms and basically obtained the same energetic order as in Refs. 24–26, see Fig. 1 where the surface formation energies of some of the studied reconstructions are plotted versus the Si chemical potential according to Eq. (1). The energy differences between different surface models are in good agreement with the predictions of *ab initio* calculations. Surface structures with Si adatoms are always energetically favored over those with C adatoms. In particular, in agreement with the *ab initio* predictions a configuration with Si adatoms on T4 places turns out to have the lowest formation energy over a wide range of variation of the Si chemical potential. Under very rich Si-growth conditions a Si3(T4) trimer configuration has, however, a slightly lower energy.

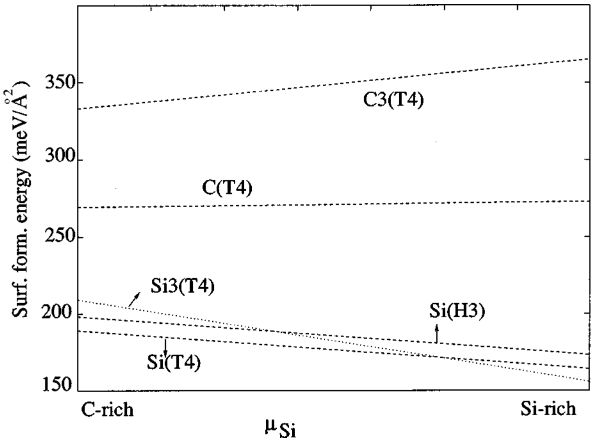

FIG. 1. Formation energies as a function of the Si chemical potential for surface reconstructions in (111) β-SiC at Si termination. The Si chemical potential μ_{Si} ranges from $\Delta H-\mu^{\mathrm{bulk}}_{\mathrm{Si}}$ to $\mu^{\mathrm{bulk}}_{\mathrm{Si}}$, where for the SiC formation energy ΔH we take the experimental value of 0.7 eV.

TABLE II. Structural parameters of the reconstructions on the Si-terminated (100) surface. The AUDD model evolves into an asymmetric dimer configuration with $c(4\times2)$ symmetry but with a slightly smaller dimer buckling. Since in the calculations by Yan, Smith, and Jonsson the (2×1) surface transforms into a pattern with $p(2\times2)$ symmetry, the dimer bond length and buckling height shown below refer to the latter one.

	(100)-Si-terminated surface		
	$d_{\text{Si-Si}}$ (Å)	Δz(Å)	Method
$c(4\times2)$	2.544	0.29	SCC-DFTB
$c(4\times2)$ (AUDD) (Ref. 43)	2.547	0.26	SCC-DFTB
4×1	2.68	0.035	SCC-DFTB
2×1	2.56	0.15	SCC-DFTB
	2.73	0.0	*ab initio* (Ref. 21)
	2.75	0.0	*ab initio* (Ref. 19)
	2.26	0.05	*ab initio* (Ref. 27) *ab initio* (Ref. 23) $[p(2\times2)]$
	2.58	0.0	*ab initio* (Ref. 22)
	2.46		Tersoff potential (Ref. 44)
	2.16		ASED (Ref. 10)

IV. RESULTS

We now turn to the reconstructions at the (100) Si-terminated surface. Following recent experimental and theoretical work (see Introduction) we consider models with 2×1, $c(4\times2)$, 4×1, 3×2, and 2×3 periodicities.

(100) Si termination

Experimentally, the $c(4\times2)$ and the 2×1 reconstructions have been found.[36] While the $c(4\times2)$ appears in well-formed surfaces, the 2×1 structure is now conceived as being related to a high density of defects. For completeness we also have investigated a configuration with 4×1 symmetry and a recently proposed new alternatively up- and down-dimer model. (AUDD model[43]) for the $c(4\times2)$ reconstruction consisting of symmetric dimers which are displaced up and down along the surface normal to form a 4×2 pattern. Dimer bond lengths of the resulting structures are listed in Table II and compared with those obtained by other approaches.

Starting from the unreconstructed 1×1 surface, in our calculations it turns out to be metallic and the same is true for exactly symmetric dimer rows. As a consequence, in such a case energy may be gained by favoring a Jahn-Teller distortion (making the dimers asymmetric and inducing a charge transfer from the lower- to the upper-lying Si atom, as a Mulliken population analysis shows), which lifts the Fermi level degeneracy, thus leading to an opening of a gap in the electronic spectrum.

This result disagrees with the *ab initio* calculations in Ref. 21, where the unreconstructed 1×1 surface proves to be semiconducting. Thus, only a comparatively small relaxation is needed in order to further stabilize the surface. This is the reason the authors only find a very weak dimerization of the surface atoms.

We particularly observed a difference in the obtained dimer bond lengths. The 2×1 and $c(4\times2)$ reconstructions show almost the same dimer lengths, 2.56 Å and 2.54 Å, respectively, values which are similar to that reported by Catellani, Galli, and Gygi,[22] $d_{\text{Si-Si}}\sim2.58$ Å. The Si-Si bond on the 4×1 surface, on the contrary, is strongly stretched to 2.68 Å, which is quite close to the results of Sabisch *et al.*[21] and Wenzien, Käckell, and Bechstedt.[18] Furthermore, the symmetric dimers of the AUDD model become asymmetric upon relaxation, still retaining the 4×2 symmetry with basically the same Si-Si bond length (2.547 Å) as in the $c(4\times2)$ configuration mentioned above. The instability of the AUDD model has also been recently supported by the *ab initio* calculations of Lu, Krüger, and Pollmann.[23]

The obtained buckling heights are substantially spread in their values: while they are relatively large, 0.19, 0.29, and 0.26 Å for the 2×1, $c(4\times2)$, and AUDD structures, respectively, the surface dimers are only buckled slightly ($\Delta z\sim0.035$ Å) in the 4×1 cell.

The results of semiempirical methods yield, when comparing to our calculations, in most cases symmetric and systematically shorter dimers, ranging from 2.16 Å [atomic-superposition and electron-delocalization (ASED) techniques[10]] to 2.46 Å [Tersoff potentials[44] and modified neglect of differential overlap (MNDO) calculations on the *PM*3-level.[11] The *ab initio* calculations of Yan, Smith, and Jonsson[27] surprisingly support the semiempirical results of the short Si dimer lengths of 2.26 Å. However, the initial structure with rows of symmetric dimers arranged in a 2×1 pattern they start from changes after relaxation into a $p(2\times2)$ configuration of slightly asymmetric dimers ($\Delta z\sim0.05$ Å). On the contrary, from DFT-LDA calculations, the dimers are expected to be quite long and symmetric, $d_{\text{Si-Si}}\sim2.73$–2.75 Å. The results of Catellani, Galli, and Gygi[22] also point in this direction.

The energy differences between the reconstructions are only a few meV, so that a clear energetic order is quite difficult to specify. This fact combined with quite differently obtained geometries indicate that the energy hypersurface for these (100)-type reconstructions is so flat that the results may be sensitive to the computational scheme used.

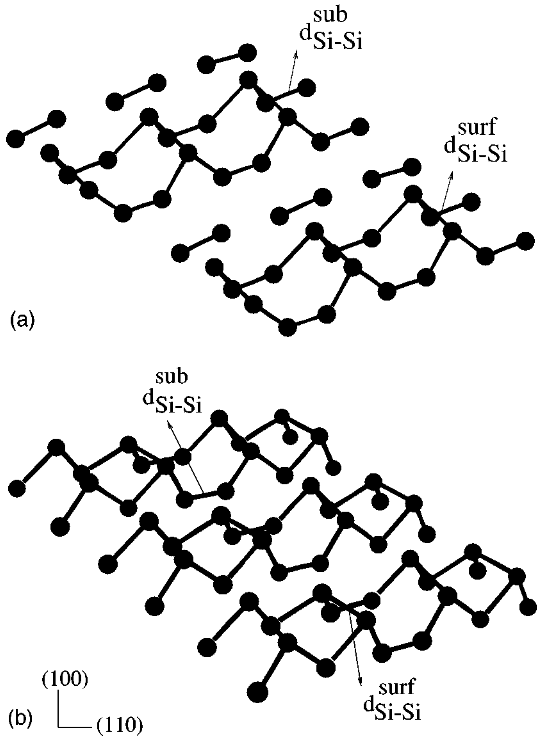

FIG. 2. Si-rich SiC(100) surface reconstructions. Note that the ADR model actually has 2×3 symmetry.

In the presence of excess silicon the most stable structures reported experimentally are 3×2, 5×2, and 7×2 surface cells.[28,29,32,34,43] Concerning the 3×2 surface a missing dimer-row (MDR) model with a silicon coverage of 2/3 was early proposed by Dayan[34] by analyzing LEED and Auger-electron spectroscopy results, see Fig. 2(b). It did not, however, correlate with other experiments, indicating that the excess silicon coverage is a 1/3 monolayer (see Ref. 36 for a review). Molecular dynamics simulations carried out by Kitabatake and Greene[15] on the basis of empirical Tersoff potentials indicated, however, that the MDR model is a low-energy configuration. Furthermore, recent core-level photoemission[35] measurements again give some support to it.

Two other surface models have still been suggested by Yan, Smith, and Jonsson [27] and Semond *et al.* [43] [alternate dimer-row (ADR) model], and Hara *et al.*[33] [added dimer-row (ADDR) model], both having a 1/3 silicon coverage. These authors favor the ADR model to be about 3.58 eV/ad-dimer lower in energy than the ADDR configuration. Although Yan, Smith, and Jonsson[27] label the ADR model as 3×2, it should be noted that it actually has a 2×3 symmetry as pointed out, e.g., in Ref. 45.

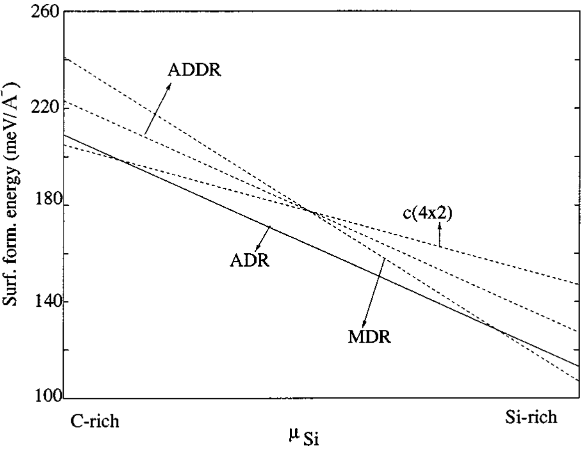

FIG. 3. Surface formation energy as a function of the Si chemical potential for different models of the 3×2 reconstruction (Si-rich surface) in (100) β-SiC. For comparison we also show the formation energy of the $c(4\times2)$ Si-terminated surface. The range of variation of μ_{Si} is the same as in Fig. 1.

In Fig. 3 we show the calculated surface formation energy for these three models as a function of the Si chemical potential. For comparison the formation energy of the previously discussed clean $c(4\times2)$ Si-terminated surface is also shown. The ADR model in our calculation has the lowest surface formation energy over a wide range of the Si chemical potential. The MDR model of Dayan is less stable than the ADR structure with the exception of a small region under very Si-rich growth conditions where it becomes energetically more favorable than the ADR configuration. The ADDR model is energetically quite unfavorable. Under Si-rich conditions it lies about 15 meV/Å^2 higher in energy than the ADR and about 10–14 meVÅ^2 above Dayan's model. Under low Si-growth conditions both the ADR and MDR models become increasingly unfavorable and a surface with $c(4\times2)$ symmetry has then the lowest formation energy, as expected.

We will now consider some structural details of these models. Since the ADDR model turns out to be energetically unfavorable we only discuss the structural properties of the ADR and MDR configurations. Some relevant structural parameters are displayed in Table III. Let us first discuss the ADR configuration, Fig. 2(a). According to Ref. 27 the added dimers are highly asymmetric ($\Delta z_{surf}\sim0.52$ Å) and very strongly bonded ($d^{surf}_{Si-Si}=2.28$ Å). Our calculations, on

TABLE III. Structural parameters of 3×2 reconstructions on the Si-rich (100) surface. For notatons see Fig. 2.

	(100)-Si-rich surface				
	d^{surf}_{Si-Si} (Å)	d^{sub}_{Si-Si} (Å)	Δz_{surf} (Å)	Δz_{sub} (Å)	Method
2×3 alternate dimer-row model (Ref. 27)	2.36	2.52/2.41	0.38	0.02	SCC-DFTB
	2.28	2.60/2.75	0.52	0	*ab initio* (Ref. 27)
3×2 missing dimer-row model (Refs. 29 and 34)	2.357/2.452	2.41	0.34/0.28	0.02	SCC-DFTB

the other side, yield a dimer length of 2.36 Å and a buckling of 0.38 Å indicating a weaker asymmetry of the dimers yet in any case stronger than in the ADDR model. The backbonds connecting the added dimers and sublayer dimers are 2.47 Å, and 2.38 Å for the higher and lower positioned added dimers atoms. Both values exceed those reported in Ref. 27, where 2.40 Å and 2.32 Å have been listed. The lengths of the sublayer dimers are 2.52 Å, and 2.40 Å, indicating stronger Si-Si bonds than obtained within the *ab initio* scheme, 2.75 Å and 2.60 Å. Furthermore, these dimers are almost symmetric, $\Delta z \sim 0.02$ Å. The isolated subsurface dimers show a buckling of $\Delta z \sim 0.19$ Å and a Si-Si bond at 2.60 Å which is weak compared to the much smaller value of 2.29 Å obtained by Yan, Smith, and Jonsson.

Consider now the MDR model of Dayan, Fig. 2(b). While in the original structure the dimers formed by the adatoms are all symmetric,[34,29] they now become asymmetric after relaxation, and pairs of adjacent dimers along the (110) direction develop an alternating buckling with two different dimer lengths: 2.35 Å and 2.45 Å and related different buckling heights Δz_{surf} of 0.34 Å and 0.28 Å, respectively. At places where adatoms are missing, almost symmetric subsurface dimers ($\Delta z_{\mathrm{surf}} = 0.02$ Å) are formed developing rows at a length of 2.41 Å, which is also in contrast to the original Dayan model, where no subsurface dimerization was postulated. The backbonds of all subsurface atoms to the carbon atoms are only slightly larger than in the bulk, 1.90–1.91 Å, indicating a very weak relaxation of the substrate. The semiempirical results of Kitabatake and Greene[15] also support the formation of asymmetric added dimers although they do not apparently show the alternating buckling found by us.

In summary, we have presented an investigation of Si-terminated surface reconstructions in SiC using a self-consistent-charge density-functional based tight-binding approach. The full-coverage (100) Si-terminated surface is stabilized by the formation of asymmetric dimer rows. The assertion of *ab initio* calculations that by the 2×1 reconstruction no dimerization would occur could not be confirmed, although the obtained bond lengths indicate a weaker Si-Si bonding than that usually obtained by semiempirical methods. For Si-rich surfaces the alternate dimer-row model proposed by Yan, Smith, and Jonsson possesses the lowest energy over a wide range of growth conditions. However, a modified Dayan model becomes energetically more favorable under very Si-rich growth conditions.

ACKNOWLEDGMENTS

We gratefully acknowledge support obtained from the Deutsche Forschungsgemeinschaft. We thank M. Lübbe for useful discussions.

---

[1] See, e.g., *Amorphous and Crystalline Silicon Carbide*, edited by C. Y.-W. Yang, M. M. Rahman, and G. L. Harris (Springer Verlag, Berlin, 1992), Vol. 4.

[2] K. J. Chang and M. L. Cohen, Phys. Rev. B **35**, 8196 (1987).

[3] C. Cheng, R. J. Needs, and V. Heine, J. Phys. C **21**, 1049 (1988).

[4] W. R. L. Lambrecht, B. Segall, M. Methfessel, and M. van Schilfgaarde, Phys. Rev. B **44**, 3685 (1991).

[5] B. Wenzien, P. Käckel, and F. Bechstedt, Surf. Sci. **307**, 989 (1994).

[6] B. I. Craig and P. V. Smith, Surf. Sci. **233**, 255 (1990).

[7] T. Halicioglu, Phys. Rev. B **51**, 7217 (1995).

[8] D. H. Lee and J. D. Joannopoulos, J. Vac. Sci. Technol. **21**, 351 (1982).

[9] T. Takai, T. Halicioglu, and W. A. Tiller, Surf. Sci. **164**, 341 (1985).

[10] S. P. Mehandru and A. B. Anderson, Phys. Rev. B **42**, 9040 (1990).

[11] P. Badziag, Phys. Rev. B **44**, 11 143 (1991).

[12] X. Hu, H. Yan, M. Kohyama, and F. S. Ohuchi, J. Phys.: Condens. Matter **7**, 1069 (1995).

[13] B. I. Craig and P. V. Smith, Surf. Sci. Lett. **256**, L609 (1991).

[14] X. Luo, G. Qian, W. Fei, E. G. Wang, and C. Chen, Phys. Rev. B **57**, 9234 (1998).

[15] M. Kitabatake and J. E. Greene, Jpn. J. Appl. Phys., Part 1 **35**, 5261 (1996).

[16] B. Wenzien, P. Käckell, and F. Bechstedt, Surf. Sci. **307**, 989 (1994).

[17] B. Wenzien, P. Käckell, and F. Bechstedt, Surf. Sci. **331**, 1105 (1995).

[18] B. Wenzien, P. Käckell, and F. Bechstedt, in *International Conference on the Physics of Semiconductors, ICPS-22, Vancouver*, 1994 (World Scientific, Singapore, 1995).

[19] P. Käckell, J. Furthmüller, and F. Bechstedt, International Conference on the Formation of Semiconductor Interfaces [Appl. Surf. Sci. **104/105**, 45 (1996)].

[20] M. Sabisch, P. Krüger, and J. Pollmann, Phys. Rev. B **51**, 13 367 (1995).

[21] M. Sabisch, P. Krüger, A. Mazur, M. Rohlfing, and J. Pollmann, Phys. Rev. B **53**, 1 (1996).

[22] A. Catellani, G. Galli, and F. Gygi, Phys. Rev. Lett. **77**, 5090 (1996).

[23] W. Lu, P. Krüger, and J. Pollmann, Phys. Rev. Lett. **81**, 2292 (1998).

[24] M. Sabisch, P. Krüger, and J. Pollmann, Phys. Rev. B **55**, 10 561 (1997).

[25] J. E. Northrup and J. Neugebauer, Phys. Rev. B **52**, 17 001 (1995).

[26] P. Käckell, J. Furthmüller, and F. Bechstedt, Diamond Relat. Mater. **6**, 1346 (1997).

[27] H. Yan, A. P. Smith, and H. Jonsson, Surf. Sci. **330**, 265 (1995).

[28] S. Hara, T. Meguro, Y. Aoyagi, M. Kawai, S. Misawa, E. Sakuma, and S. Yoshida, Thin Solid Films **225**, 240 (1993).

[29] S. Hara, S. Misawa, S. Yoshida, and Y. Aoyagi, Phys. Rev. B **50**, 4548 (1994).

[30] V. M. Bermudez and R. Kaplan, Phys. Rev. B **44**, 11 149 (1991).

[31] T. Fuyuki, T. Yoshinobu, and H. Matsunami, Thin Solid Films **225**, 225 (1993).

[32] R. Kaplan, Surf. Sci. **215**, 111 (1989).

[33] S. Hara, W. F. J. Slijkerman, J. F. van der Veen, I. Ohdomari, S.

Misawa, E. Sakuma, and S. Yoshida, Surf. Sci. **231**, L196 (1990).

[34] M. Dayan, J. Vac. Sci. Technol. A **4**, 38 (1986).

[35] H. W. Yeom, Y.-C. Chao, S. Terada, S. Hara, S. Yoshida, and R. I. Uhrberg, Phys. Rev. B **56**, R15 525 (1997).

[36] V. M. Bermudez, Phys. Status Solidi B **202**, 447 (1997).

[37] V. V. Elsbergen, T. U. Kampen, and W. Mönch, Surf. Sci. **365**, 443 (1996).

[38] L. Li, Y. Hasegawa, and T. Sakurai, J. Appl. Phys. **80**, 2524 (1996).

[39] P. Martensson, F. Owman, and L. I. Johansson, Phys. Status Solidi B **202**, 501 (1997).

[40] D. Porezag, Th. Frauenheim, Th. Köhler, G. Seifert, and R. Kaschner, Phys. Rev. B **51**, 12 947 (1995).

[41] M. Elstner, D. Porezag, G. Jungnickel, J. Elsner, M. Haugk, Th. Frauenheim, S. Suhai, and G. Seifert, Phys. Rev. B **58**, 7260 (1998).

[42] G. X. Quian, R. M. Martin, and D. J. Chadi, Phys. Rev. B **38**, 7649 (1988).

[43] F. Semond, P. Soukiassian, A. Mayne, G. Dujardin, L. Douillard, and C. Jaussaud, Phys. Rev. Lett. **77**, 2013 (1996).

[44] H. Yan, X. Hu, and H. Jonsson, Surf. Sci. **316**, 81 (1994).

[45] M. Lübbe, K. Lindner, S. Sloboshanin, S. Tautz, J. Schäfer, and D. R. T. Zahn (unpublished).